



Competitive metal–ligand binding between CdTe quantum dots and EDTA for free Ca²⁺ determination



S. Sofia M. Rodrigues^a, Diego R. Prieto^b, David S.M. Ribeiro^{a,*}, Enrique Barrado^b, João A.V. Prior^a, João L.M. Santos^{a,*}

^a REQUIMTE, Department of Chemical Sciences, Laboratory of Applied Chemistry, Faculty of Pharmacy, University of Porto, Rua de Jorge Viterbo Ferreira no. 228, 4050-313 Porto, Portugal

^b QUIANE, Department of Analytical Chemistry, Faculty of Sciences, University of Valladolid, Paseo de Belén 7, 47011 Valladolid, Spain

ARTICLE INFO

Article history:

Received 15 September 2014

Received in revised form

30 October 2014

Accepted 4 November 2014

Available online 13 November 2014

Keywords:

Calcium

Quantum dots

EDTA

Multipumping flow system

Photoluminescence quenching

ABSTRACT

In this work, a fluorometric approach for the selective determination of calcium by using CdTe nanocrystals as chemosensors, was developed. The quantum dots interacted not with the metal, but with a ligand that also bonded the metal. The fluorescence response was modulated by the extension of the competitive metal–ligand binding, and therefore the amount of free ligand. CdTe quantum dots (QDs) with different capping layers were evaluated, as the QDs surface chemistry and capping nature affected recognition, thus the magnitude of the ensuing fluorescence quenching. The developed procedure was automated by using a multipumping flow system.

Upon optimization, thioglycolic acid (TGA) and EDTA were selected as capping and ligand, respectively, providing a linear working range for calcium concentrations between 0.80–3.20 mg L⁻¹, and a detection limit of 0.66 mg L⁻¹. A quenching mechanism relying on nanocrystal destabilization upon detachment of surface Cd by the ligand was proposed.

© 2014 Elsevier B.V. All rights reserved.

1. Introduction

Calcium is one of the most common naturally occurring metal ion in minerals and natural waters, with a decisive contribute to water total hardness and potability [1]. Although not posing any health treat, high calcium contents could engage in reactions that lead to the formation of insoluble mineral deposits, which could dramatically reduce the efficiency of heat transfer, with a corresponding increase in the industry operational costs, or act as water flow obstructions that are only solved upon replacement of the affected parts. For this reason, routine quality control of calcium in drinking and industrial waters is required.

Most of the analytical methodologies that have been proposed for calcium determination rely on potentiometry [2–4], atomic absorption spectroscopy [5], ion chromatography [6,7] and high-performance liquid chromatography [8]. These methods exhibited strengths, such as good precision and high sensitivity, but also some weaknesses as they require expensive equipment, skilled operators and laborious or specific sample pre-treatments. A few

colorimetric methods involving the formation of colored calcium complexes using metallochromic reagents, such as, 4-(2-pyridylazo)resorcinol [9], glyoxal bis(2-hydroxyanil) [10], 3,3'-bis[*N,N*-bis(carboximethyl)aminomethyl]-*o*-cresolphthalein [11], arsenazo (III) [12], methylthymol blue [13] and alizarin red sulphionate (ARS) [14], have also been reported. Nevertheless, most of these chromogenic reagents present some shortcomings with respect to selectivity, sensitivity and reaction pH.

Notwithstanding the numerous methodologies already developed for calcium determination in waters, a significant number of routine laboratories resorts to complexometric methods employing EDTA as complexant and murexide or Eriochrome Black T as indicator [1]. Although providing cost-effective results, complexometric determinations are time-consuming and subject to operational errors due to the difficulties associated to end-point detection.

Fluorometric methods can be used as suitable alternatives for the detection of metal ions because of their attractive advantages, such as, high sensitivity, selectivity and simplicity. In general, a fluorescent chemosensor for metal species interacts directly the metal ion in solution signalling the recognition event by a change in the fluorescence properties such as the emission wavelength or intensity. Herein, the chemosensor interacts not with the metal, but with a ligand that also binds the metal. The fluorescence

* Corresponding authors.

E-mail addresses: dsmribeiro@gmail.com (D.S.M. Ribeiro), joalms@ff.up.pt (J.L.M. Santos).

response is modulated by the extension of the competitive metal–ligand binding, and therefore the amount of free ligand.

Concerning the development of new fluorometric chemosensors, quantum dots (QDs) have acquired in recent years a noteworthy relevance as valuable alternatives to the traditional organic fluorophores. QDs are colloidal semiconductor nanocrystals with remarkable optical and chemical properties that include broad absorption profiles, size-tunable narrow photoluminescence, high quantum yields and long-term photostability [15], etc. QDs analytical potential is undoubtedly related with their photoluminescence (PL) and reactivity, which could be exploited through the manipulation of their surface chemistry by controlling the nanocrystal size, morphology and surface capping ligands [16]. The selection of a suitable capping is of primordial importance because it determines not only the adequate solubility of quantum dots in the dispersion media but also dictates the selectivity and the sensitivity of the nanoparticles for a target analyte [17]. Effectively, depending on the analyte-targeting strategy some characteristics such as capping reactivity, capping thickness and surface charges should be taking into consideration.

A few works have evaluated the interaction of quantum dots surface with different chelating agents, such as, phenanthroline (Phen) [18,19], ammonium pyrrolidine dithiocarbamate (APDC) [20] and ethylenediaminetetraacetic acid (EDTA) [21,22], which generally induced inhibition of the nanocrystals photoluminescence. In these works QDs PL quenching was ascribed to a photoinduced hole transfer (PHT) process from QDs to Phen [18,19] and to a ligand-depletion process in which APDC and EDTA were used as chemical etching reagents [20–22].

Herein, and for the first time, a thorough study of the surface interactions between EDTA and CdTe nanocrystals capped with five different thiol-ligands, namely, thioglycolic acid (TGA), 3-mercaptopropionic acid (MPA), glutathione (GSH), cysteine (CYS) and 2-mercaptoethanesulfonate (MES) was carried out. In simultaneous, a chemosensor based on the EDTA-induced fluorescent quenching of QDs was developed for calcium determination in drinking waters. The proposed analytical methodology relied on the preventing effect of Ca^{2+} on the PL quenching of QDs induced by EDTA, and was automated by exploiting the resourceful operational characteristics of multipumping flow systems (MPFS) [23]. Reproducible and individual control of each reagent solution in combination with the fluid dynamics of the pulsed streams generated by each micro-pump actuation promoted a fast and efficient mixture of sample and reagents, and consequently an adequate reaction development with stable readouts even without reaching equilibrium conditions. This feature allows circumventing the main drawback of the commonly used batch procedures, which, by demanding the attainment of long-lasting chemical equilibrium conditions for the obtaining of stable photoluminescence readouts are frequently affected by nanoparticles solution stability problems [15] that totally impair detection and measurements.

2. Experimental

2.1. Apparatus

In the flow manifold designed for this work, four 120SP solenoid micro-pumps (Bio-Chem Valve Inc. Boonton, NJ, USA) delivering 10 μL per stroke were used as the only active devices for the insertion and propulsion of the solutions. These solenoid devices were controlled through a homemade power drive based on the ULN2003 chip linked to the microcomputer parallel port. To this end, the software was developed in Microsoft Visual Basic 6.0[®].

The different components of the flow system were connected with 0.8 mm i.d. polytetrafluoroethylene PTFE tubing (Omnifit,

Cambridge, UK), lab-made end-fittings, connectors and acrylic confluence points.

The detector was a spectrofluorometer, Jasco (Easton, MD, USA), model FP-2020/2025, equipped with a flow cell with an internal volume of 16 μL . The analytical signals were recorded on a strip chart recorder, model Linseis L 250E (Robbinsville, NJ, USA).

The nanoparticles were characterized through a UV–vis Jasco V-660 spectrophotometer (Easton, MD, USA) and a LS-50B Perkin Elmer spectrofluorometer (Waltham, MA, USA) for obtaining the QDs absorption and emission spectra, respectively.

For the separation of the precipitated nanocrystals, a Thermo-Electron Jouan BR4I refrigerated centrifuge (Waltham MA, USA) was used.

X-ray powder diffraction (XRD) studies of the synthesized nanocrystals were performed using a Philips X'Pert X-ray MPD diffractometer (Cu $K\alpha$ radiation). A scan rate of 40.0 s for step at step intervals of 0.04° was used for XRD data collection.

2.2. Samples, standards and reagents

All solutions used in this work were prepared using water purified from a Milli-Q system (conductivity $\leq 0.1 \mu\text{S cm}^{-1}$). Chemicals were all of analytical reagent grade without any treatment process or further purification.

Several QDs and EDTA solutions were tested in different pH media by using $\text{KH}_2\text{PO}_4/\text{NaOH}$ (pH=7), $\text{H}_3\text{BO}_3/\text{KCl}/\text{NaOH}$ (pH=9) and $\text{Na}_2\text{HPO}_4/\text{NaOH}$ (pH=11 and 12) buffers, which were prepared according to Perrin et al. [24]. Sodium hydroxide ($\geq 98\%$), potassium chloride ($\geq 99.0\%$), boric acid ($\geq 99.5\%$), potassium phosphate monobasic ($\geq 99.0\%$) and sodium phosphate dibasic anhydrous ($\geq 99.0\%$) were all purchased from Sigma-Aldrich (St. Louis, MO, USA).

For Ca^{2+} determination assays, a stock solution containing 1.00 $\mu\text{mol L}^{-1}$ of TGA-capped CdTe QDs was prepared by dissolving 4.00 mg of the synthesized and purified nanoparticle, with a size of 2.32 nm, in 25 mL of boric acid/KCl/NaOH buffer pH=9. Then, a solution of 0.025 $\mu\text{mol L}^{-1}$ of TGA–CdTe QDs were daily prepared by proper dilution of the above stock solution into a 25.00 mL volumetric flask and the volume was completed to the mark with boric acid/KCl/NaOH buffer pH=9.

A ethylenediaminetetraacetic acid stock solution of $1.0 \times 10^{-3} \text{ mol L}^{-1}$ was prepared by dissolving 18.61 mg of EDTA (Sigma-Aldrich, St. Louis, MO, USA) in 50 mL of boric acid/KCl/NaOH buffer pH=9. For the assays, a EDTA solution with a concentration of $4.0 \times 10^{-5} \text{ mol L}^{-1}$ was daily prepared by appropriate dilution of the stock solution in 100 mL volumetric flask with boric acid/KCl/NaOH buffer solution at pH=9.

A 400 mg L^{-1} calcium stock solution was prepared by dissolving 73.5 mg of $\text{CaCl}_2 \cdot 2\text{H}_2\text{O}$ (Sigma-Aldrich, > 98%, St. Louis, MO, USA) in 50 mL of boric acid/KCl/NaOH buffer solution at pH=9.

The working calcium standard solutions (0.80–3.20 mg L^{-1}) were daily prepared by appropriate dilution of the $\text{CaCl}_2 \cdot 2\text{H}_2\text{O}$ stock solution by transferring aliquots (50–200 μL) into a series of 25 mL volumetric flasks and the volume was made up to the mark with boric acid/KCl/NaOH buffer solution at pH=9.

Six mineral water samples commercially available in Spain, were analyzed according to the proposed method without any pre-treatment. All samples were prepared by diluting with boric acid/KCl/NaOH buffer solution at pH=9, in 25 mL volumetric flasks, an appropriate volume of the mineral water aiming to obtain a calcium content within the working range of the analytical procedure.

2.3. Reagents and synthesis of CdTe quantum dots

For the synthesis of the CdTe quantum dots, cadmium chloride hemi(pentahydrate) ($\text{CdCl}_2 \cdot 2.5\text{H}_2\text{O}$, 99%), sodium telluride (100 mesh,

99%), tellurium powder (200 mesh, 99.8%), sodium borohydride (NaBH_4 , 99%), L-glutathione reduced ($\geq 98\%$), L-cysteine ($\geq 97\%$), sodium 2-mercaptoethanesulfonate ($\geq 98.0\%$) and thioglycolic acid ($\geq 98\%$) were purchased from Sigma-Aldrich (St. Louis, MO, USA). Trisodium citrate dehydrate and 3-mercaptopropionic acid (99%) were obtained from Fluka (St. Louis MO, USA). Absolute ethanol (99.5%) was purchased by Panreac (Barcelona, Spain).

CdTe nanocrystals were synthesized using L-glutathione reduced (GSH), 3-mercaptopropionic acid (MPA), L-cysteine (CYS), sodium 2-mercaptoethanesulfonate (MES) and thioglycolic acid (TGA) as stabilizing agents in aqueous solution. GSH-capped CdTe QDs were prepared in a one-step route by modified Qian's procedure [25]. Briefly, CdCl_2 , Na_2TeO_3 and GSH (Cd:Te:GSH molar ratio 1:0.2:1.2) were added into a single reaction pot with NaBH_4 , trisodium citrate and water. The solution pH was adjusted to 10.5 by the addition of 1.0 mol L^{-1} NaOH and the resulting solution was heated with vigorous stirring at 100°C under reflux for QDs growth. MPA [26], CYS, TGA [27] and MES-capped QDs [unpublished results] were synthesized by using CdCl_2 and NaHTe as precursors. Briefly, the first stage consists on the reduction of tellurium with NaBH_4 in N_2 saturated water to produce NaHTe [28]. For MPA-coated QDs, after all tellurium has been completely consumed the resulting solution was transferred to another flask containing $4.0 \times 10^{-3} \text{ mol}$ of CdCl_2 and $6.8 \times 10^{-3} \text{ mol}$ of MPA in 100 mL N_2 saturated solution. The pH of the solution was adjusted to 11.5 by the addition of 1.0 mol L^{-1} NaOH solution. The molar ratio of Cd:Te:MPA was fixed at 1:0.1:1.7. The size of CdTe QDs was tuned by changing the refluxing time. CYS, TGA and MES-coated QDs were synthesized by using the same procedure, at pH 10.5, 11.0 and 11.7, respectively and Cd:Te:CYS/TGA/MES molar ratios of 1:0.1:4.6 for TGA and 1:0.05:2.4 for CYS and MES-capped nanocrystals.

To purify the prepared QDs crude solutions were precipitated in absolute ethanol [29] to remove the excess of reactants and the precipitates was subsequently separated by centrifugation, vacuum dried, kept in amber flasks and protected from light, for posterior use. QDs solutions were daily prepared by dissolving a certain amount of the dried nanocrystals in ultrapure water or different buffers solutions at the desired concentration for the surface conjugation.

2.4. MPFS manifold and analytical procedure

Concerning the reaction scheme involved in the fluorometric determination of calcium, the flow manifold was configured (Fig. 1) to allow the merging of the sample (Ca^{2+}) and the EDTA streams creating a first reaction zone. Subsequently, the developing reaction

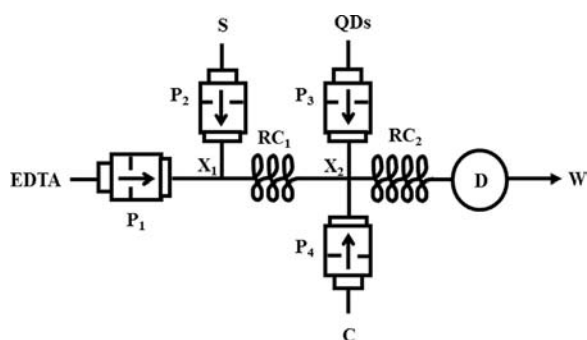


Fig. 1. Flow diagram for the determination of calcium. EDTA, ethylenediaminetetraacetic acid prepared in boric acid/KCl/NaOH buffer solution at pH=9; S, sample solution prepared in boric acid/KCl/NaOH buffer pH=9; QDs, TGA-capped CdTe quantum dots prepared in boric acid/KCl/NaOH buffer solution at pH=9; C, carrier solution, boric acid/KCl/NaOH buffer solution at pH=9; W, waste; P_1 – P_4 , solenoid micro-pumps (internal volume $10 \mu\text{L}$); X_1 – X_2 , confluence points; RC_1 , 50-cm reactor; RC_2 , 100-cm reactor; D, fluorometer detector ($\lambda_{\text{ex}}=400 \text{ nm}$ and $\lambda_{\text{em}}=534 \text{ nm}$).

mixture was merged with QDs stream creating a second reaction zone. This way, only the excess of free EDTA will react with QDs avoiding the possible interference of Ca^{2+} in the photoluminescence properties of the nanoparticles.

Before the beginning of each analytical cycle, all flow tubing were filled with the corresponding solution by actuating the respective micro-pump. The first stage of the analytical procedure involved the insertion of sample and EDTA solutions by exploiting the merging zones approach, through the simultaneous actuation of micro-pumps P_1 and P_2 . The number of P_1 and P_2 pulses was enough to guarantee that the first reaction zone completely filled the 50-cm reactor coil (RC_1) positioned between the confluence points X_1 and X_2 . Afterward, the micro-pump P_4 was activated and the carrier solution (boric acid/KCl/NaOH buffer solution at pH=9) was inserted into the flow system at confluence point X_2 , propelling the exceeding volumes of the first reaction zone to waste. At the same time baseline was established.

The second stage of the analytical procedure consisted in the sampling stage wherein a pre-set number of $10 \mu\text{L}$ aliquots of QDs solution were intercalated with plugs of the first reaction zone (pre-mixed sample/EDTA solution). More specifically, through the alternated activation of the micro-pumps P_1 , P_3 and P_2 , in this order, one pulse of QDs solution was inserted between two pulses of the first reaction zone, which was repeated for a pre-selected number of times defining thus the volumes of reagents and sample solutions inserted in the flow system. Then, the micro-pumps P_1 , P_2 and P_3 were switched off and by only the repeated actuation of P_4 , the second reaction zone was transported towards detection for monitoring of the fluorescence emission at 534 nm ($\lambda_{\text{ex}}=400 \text{ nm}$). In the analytical procedure all micro-pumps were activated at a fixed pulse time of 0.2 s (which is equivalent to 0.350 s , sum of pump on/pump off time intervals) corresponding to a pulse frequency of 171 min^{-1} , establishing a flow rate of 1.71 mL min^{-1} .

2.5. Characterization of quantum dots

The optical properties of the synthesized CdTe QDs capped with different organic ligands were evaluated and characterized through the UV–vis absorption and photoluminescence spectra showed in Fig. 2. The absorbance spectra showed that the different QDs have wide absorption bands with well resolved absorption maxima for the first excitonic transition wherein the corresponding wavelengths values ranging from 496 to 510 nm (results are summarized in Table 1). Therefore, by using the obtained wavelengths of maximum absorption corresponding to the first transition (λ), the particle sizes of the QDs (D) were determined according to the empirical formula (Eq. (1)) proposed by Yu et al. [30].

$$D = (9.8127 \times 10^{-7})\lambda^3 - (1.7147 \times 10^{-3})\lambda^2 + (1.0064)\lambda - (194.84) \quad (1)$$

The diameters values of the different synthesized nanocrystals are presented in Table 1 ranging from 2.23 to 2.60 nm . It was also observed that the different nanocrystals exhibited narrow and symmetric emission spectra with maximum emission wavelengths comprised between 534 and 546 nm (Table 1). In order to evaluate size dispersion the full width at half maximum (FWHM) values of the QDs emission bands were determined. The obtained values, presented in Table 1, showed that all prepared QDs are homogeneous and nearly monodisperse.

X-ray powder diffraction was also used to obtain information about the crystal structure and to confirm the size of the QDs. Fig. 3 represents the X-ray diffraction pattern obtained for TGA-capped CdTe QDs, which showed the characteristic broad peaks of the zinc

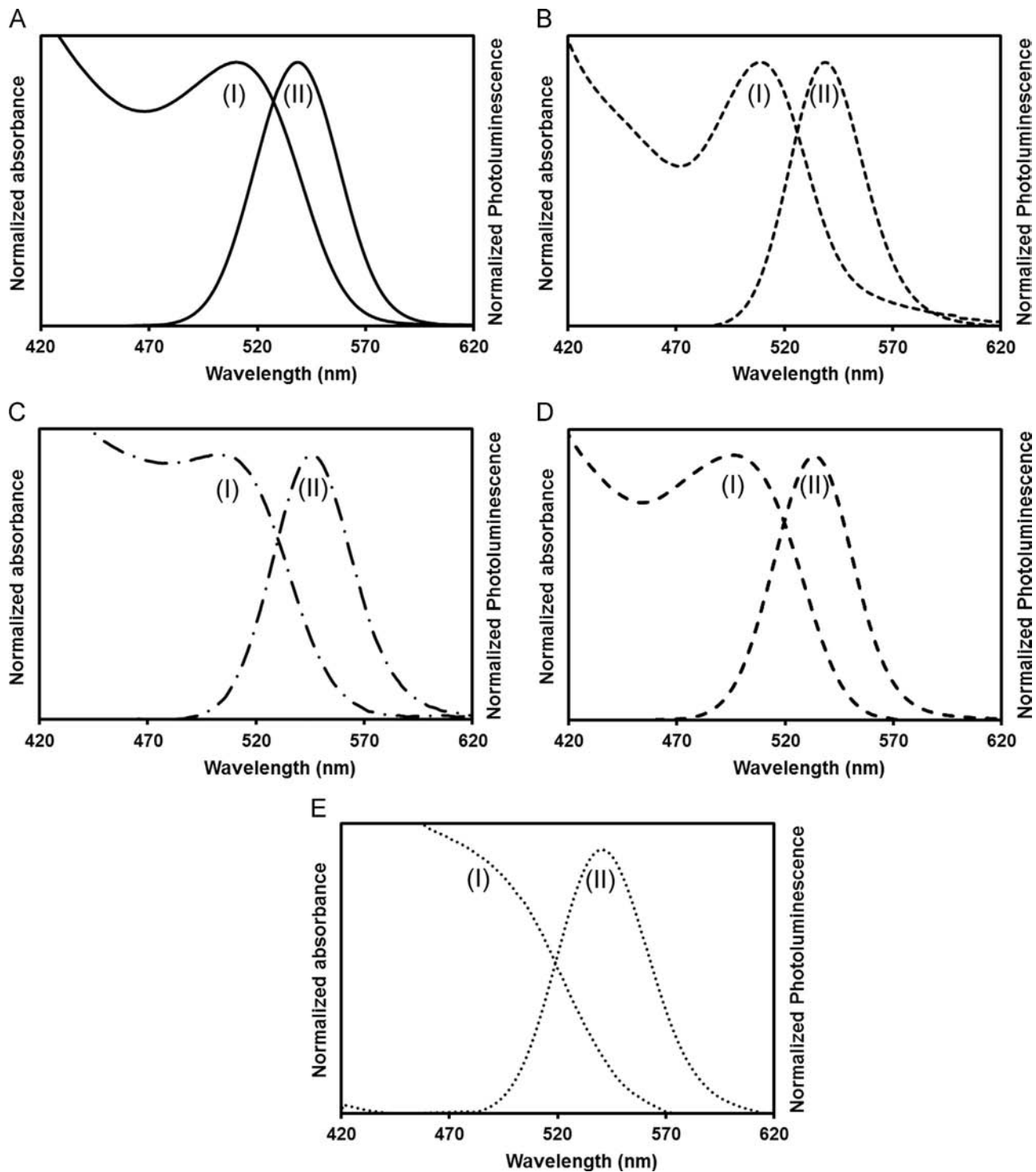


Fig. 2. (I) Normalized absorbance and (II) photoluminescence spectra of the synthesized CdTe QDs capped with different organic ligands: (A) cysteine; (B) glutathione; (C) mercaptopropionic acid; (D) thioglycolic acid; (E) mercaptoethanesulfonic acid.

blend crystalline structure that are attributed to the (1 1 1), (2 2 0), and (3 1 1) planes. Nanocrystals size was also confirmed by XRD, according to Scherrer equation (Eq. (2)):

$$D = \frac{k\lambda}{\beta \cos \theta} \quad (2)$$

wherein λ is the wavelength of the X-ray source (1.5405 Å), k is an empirical constant equivalent to 0.9, β is the full width at half maximum of the diffraction peak, and θ is the angular position. The

sizes of all synthesized nanoparticles analysed by XRD were in accordance with those estimated by using Eq. (1).

The molar concentration of the different nanocrystals needed to be calculated in order to standardize the preparation of the QDs solutions. This was accomplished through the estimation of the molar absorptivity values (ϵ) by using the formula (Eq. (3)) of Yu et al. [30], which takes into consideration the UV-vis spectra of the QDs, and by using the Lambert-Beer law:

$$\epsilon = 3450\Delta E(D)^{2.4} \quad (3)$$

Table 1

First excitonic transition ($\lambda_{1st\ exci}$) and emission (λ_{em}) wavelengths, full width at half maximum (FWHM) and diameter of the synthesized CdTe QDs capped with different organic ligands.

QD capping	$\lambda_{1st\ exci}$ (nm)	λ_{em} (nm)	FWHM (nm)	Diameter (nm)
CYS	510	539	45.6	2.60
GSH	509	539	40.3	2.57
MPA	505	546	43.2	2.48
TGA	499	534	42.6	2.32
MES	496	542	49.5	2.23

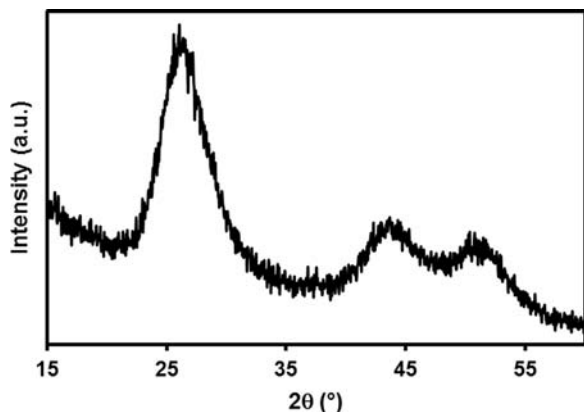


Fig. 3. p-XRD of 2.32 nm TGA capped CdTe QDs.

ΔE is the transition energy corresponding to the first absorption peak and the unit is eV.

3. Results and discussion

Quantum dots are extremely reactive nanomaterials. Nevertheless, this reactivity is to some extent susceptible of control by combining the optimum selection of the capping ligand and the nanocrystals size. The outer stabilizing capping layer surrounding the nanocrystals influences their reactivity and the stability in the solution. The use of different terminal groups of the capping ligands pointing to the outside environment provides the necessary chemical accessibility for the QDs to interact with target analytes, thus determining the selectivity and sensitivity of the reaction [15,31].

This way, taking into consideration the main goal of the developed work, some assays involving the study of the influence of different QDs capping materials were conducted. These assays were carried out by resorting to an automatic flow methodology that allowed to achieve, for all measurements, a good compromise between the QDs stability (dependent on the capping) and the target–analyte interaction process (affecting the photoluminescent properties of the nanoparticle). Considering that the QDs surface interactions with the analyte not only change the photoluminescence response but also the QDs solution stability, and since this latter issue is imperative to attain stable analytical readouts, continuous flow methodologies are attractive analytical tools for carrying out the assays. In effect, automatic flow methodologies have the advantage of allowing a reproducible solutions insertion and timed reaction development without the need for reaching chemical equilibrium conditions. Moreover, the methodology based on a multipumping approach enabled the individual control of each of the involved solutions facilitating not only the mixing of reagents and the establishment of the reaction zone but also the optimization of all the chemical and physical conditions.

3.1. Preliminary assays

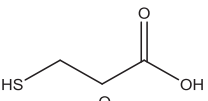
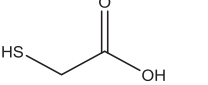
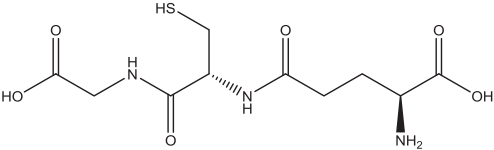
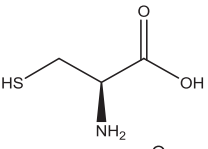
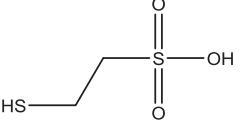
The fluorescence properties of CdTe QDs capped with different ligands (MPA, TGA, GSH, CYS and MES) were evaluated upon interaction with EDTA, at different pH values. The media pH had a strong influence in both the quantum dots stability and in the extent of the reaction with EDTA. With the purpose of conducting the preliminary assays in a reproducible way a flow-based system relying on the multipumping concept was implemented, which was able to monitor the fluorescence quenching effect (ΔF (%)) resulting from the interaction between EDTA, at several concentrations (up to $1.0 \times 10^{-3} \text{ mol L}^{-1}$), and QDs with 5 different capping ligands. In simultaneous, different pH values (7.0, 9.0, 11.0 and 12.0), were also evaluated.

This MPFS manifold comprised three solenoid actuated micro-pumps, with a stroke volume of 10 μL , a 50 cm reactor coil and a fluorescence detector. Two of the micro-pumps were responsible for the insertion of QDs and EDTA solutions, respectively, while the third one was used to propel the carrier solution (a buffer solution at each of the pH value tested). To assure that the reaction between QDs and EDTA was completed at the time of measurement of the fluorescence signal the flowing stream was halted for a stopped-flow period of 90 s prior to detection. This time value was selected upon an assay aimed at the study of the influence of increased halting periods (with 15 s increment) on the analytical signal. Despite the fact that the exploitation of an automatic flow system for analytical purposes do not imposes the completeness of the chemical reactions, in this preliminary assays it was important to assure that all possible interactions of EDTA with the MPA, TGA, GSH, CYS and MES–QDs occurred and not to be focused exclusively in the reaction kinetics.

In the global assay five solutions of CdTe–QDs with a concentration fixed at 0.1 $\mu\text{mol L}^{-1}$ were used, each one corresponding to a different capping: MPA–CdTe QDs ($\phi=2.48$ nm), TGA–CdTe QDs ($\phi=2.32$ nm), GSH–CdTe QDs ($\phi=2.57$ nm), CYS–CdTe QDs ($\phi=2.60$ nm) and MES–CdTe QDs ($\phi=2.23$ nm). The listed capping ligands, used in the QDs synthesis (Table 2), were selected according to the structure of the respective molecules, which took into account the functional groups that were present and the length of the hydrocarbon chain. Among the structural differences that are visible in the used capping ligands one can briefly mention that upon binding to the semiconductor core (through the thiol group) MPA and TGA remained with only one free functional group, in this case a carboxylic acid group, whilst CYS and GSH, showed both carboxylic and amine groups. MES molecule displayed a sulfonic acid functional group. The length of the hydrocarbon chain also varies appreciably, as can be observed in Table 2.

The preliminary studies were performed aiming at the highest photoluminescence quenching of the QDs, considered in terms of the percentage variation (ΔF (%)) of the analytical signal between the blank reading (QDs native fluorescence) and QDs fluorescence after reaction with EDTA. The results, compiled in Fig. 4 and (Table S1 Supplementary material), revealed that QDs capped with MPA and MES required higher concentrations of EDTA to attain high ΔF (%). This indicates that the sensitivity provided by these quantum dots would be relatively low, considering the high amounts of analyte that would be necessary for detection. For QDs capped with GSH it was observed that when using pH=9.0, 11.0 and 12.0, the ΔF (%) was never superior to 85%, even with high EDTA concentrations. However, for pH=7.0 a ΔF (%) of approximately 100% was obtained for a concentration of EDTA of $1.0 \times 10^{-4} \text{ mol L}^{-1}$. More revealing were the results obtained for QDs capped with CYS and TGA, which provided the highest ΔF (%) values (about 100%), even when using low EDTA concentrations. This could be an indication that, in the assayed conditions, these

Table 2
Molecular structures of the capping ligands cysteine (CYS), glutathione (GSH), mercaptopropionic acid (MPA), thioglycolic acid (TGA) and mercaptoethanesulfonic acid (MES).

Name	Molecular structure	Functional group ^a
Mercaptopropionic acid (MPA)		Carboxylic acid (-COOH)
Thioglycolic acid (TGA)		Carboxylic acid (-COOH)
Glutathione (GSH)		Carboxylic acid (-COOH) Primary amine (-NH ₂)
Cysteine (CYS)		Carboxylic acid (-COOH) Primary amine (-NH ₂)
Mercaptoethanesulfonic acid (MES)		Sulfonic acid (-SO ₂ OH)

^a Available functional groups, upon binding of the ligand thiol group to the surface of QDs.

capping ligands allowed to obtaining more reactive QDs. More specifically, the highest analytical signal was obtained when using a pH=7.0, CYS-CdTe QDs and a solution of EDTA with a concentration of $5.0 \times 10^{-5} \text{ mol L}^{-1}$. Also, for the TGA ligand, at pH=9.0 and 11.0, and a concentration of EDTA of 7.5×10^{-5} and $6.0 \times 10^{-5} \text{ mol L}^{-1}$ respectively, the ΔF (%) was superior to 97%.

It should be emphasized that at pH=7.0 all of the assayed nanomaterials exhibited a poor solution stability that was clearly perceptible through the formation of a precipitate in the QDs solutions. This phenomenon was independent of the capping ligand being more accentuated and occurring faster for GSH and CYS. This could mean that, for some of the assays, the high ΔF (%) values obtained did not result from EDTA interaction with the QDs but were instead a consequence of a photoluminescence decrease due to QDs precipitation. In order to check if the precipitation was related with the chemical composition of the buffer solution, a TRIS buffer solution at pH=7.0 was used to repeat the interaction assays between CYS-CdTe QDs and EDTA. The formation of a precipitate confirmed that both these were independent of the buffer being used and the impracticality of using a pH equal or lower than 7.0. A possible explanation is that at a pH lower than 7.0 occurs the protonation of the thiol groups of the capping ligands that consequently dissociate from the surface of the nanocrystals that become unstable and precipitate.

In line with the results obtained in the preliminary assays, the developed approach showed a noteworthy analytical potential for the determination of metallic species that could compete with the QDs for EDTA, thus preventing the QDs fluorescence quenching effect of the later.

Consequently, the succeeding assays were aimed at the optimization of the analytical system performance, seeking the highest sensitivity, for application in the determination of metallic ions in drinking water samples. Due to its relevance and predominance, and since it constitutes a very important characterization parameter of water in any laboratory analysis report, calcium was selected as model cation. Moreover, to our knowledge, this is the

first work dealing with the utilization of quantum dots for the determination of calcium. The assays were based on the reaction between TGA-CdTe QDs and EDTA, at pH=9.0 and 11.0.

3.2. Optimization of the MPFS

The proposed methodology was developed aiming at the monitoring of calcium ion in water samples with very low levels of contaminant ions. To assure enhanced versatility in terms of sample handling and processing, the methodology was automated by taking advantage of the pulsed multipumping flow system used in the preliminary assays, which was easily reconfigured by adding a supplementary micro-pump accountable for sample insertion (Fig. 1). Since the reaction medium had a strong influence on quantum dots reactivity with EDTA, the chemical and physical reaction parameters were fine-tuned using the reconfigured flow system. Nevertheless, the determination of calcium could not be accomplished by the present methodology at pH=11.0 because calcium ions precipitate in the presence of phosphate ions of the buffer solution, making the method unfeasible.

3.2.1. Optimization of the chemical parameters

Taking into consideration preliminary results, the quenching of QDs fluorescence was highly influenced by the concentration of EDTA, which was itself, as expected, dependent on the QDs concentration. This way, the optimization of the chemical conditions at pH 9.0 was carried out by using a fixed nanoparticles concentration and by evaluating the measurable quenching effect of increasing concentrations of EDTA, up to $1.75 \times 10^{-5} \text{ mol L}^{-1}$. This procedure was repeated for distinct concentrations of TGA-CdTe QDs: 0.025, 0.05, 0.1 and $0.25 \mu\text{mol L}^{-1}$. Maximum relative quenching (ΔF (%)) was obtained when using EDTA solutions with concentrations of $4.0 \times 10^{-5} \text{ mol L}^{-1}$, $6.0 \times 10^{-5} \text{ mol L}^{-1}$, $1.0 \times 10^{-4} \text{ mol L}^{-1}$ and $1.75 \times 10^{-4} \text{ mol L}^{-1}$, for QDs solutions with concentrations of 0.025, 0.05, 0.1 and $0.25 \mu\text{mol L}^{-1}$, respectively.

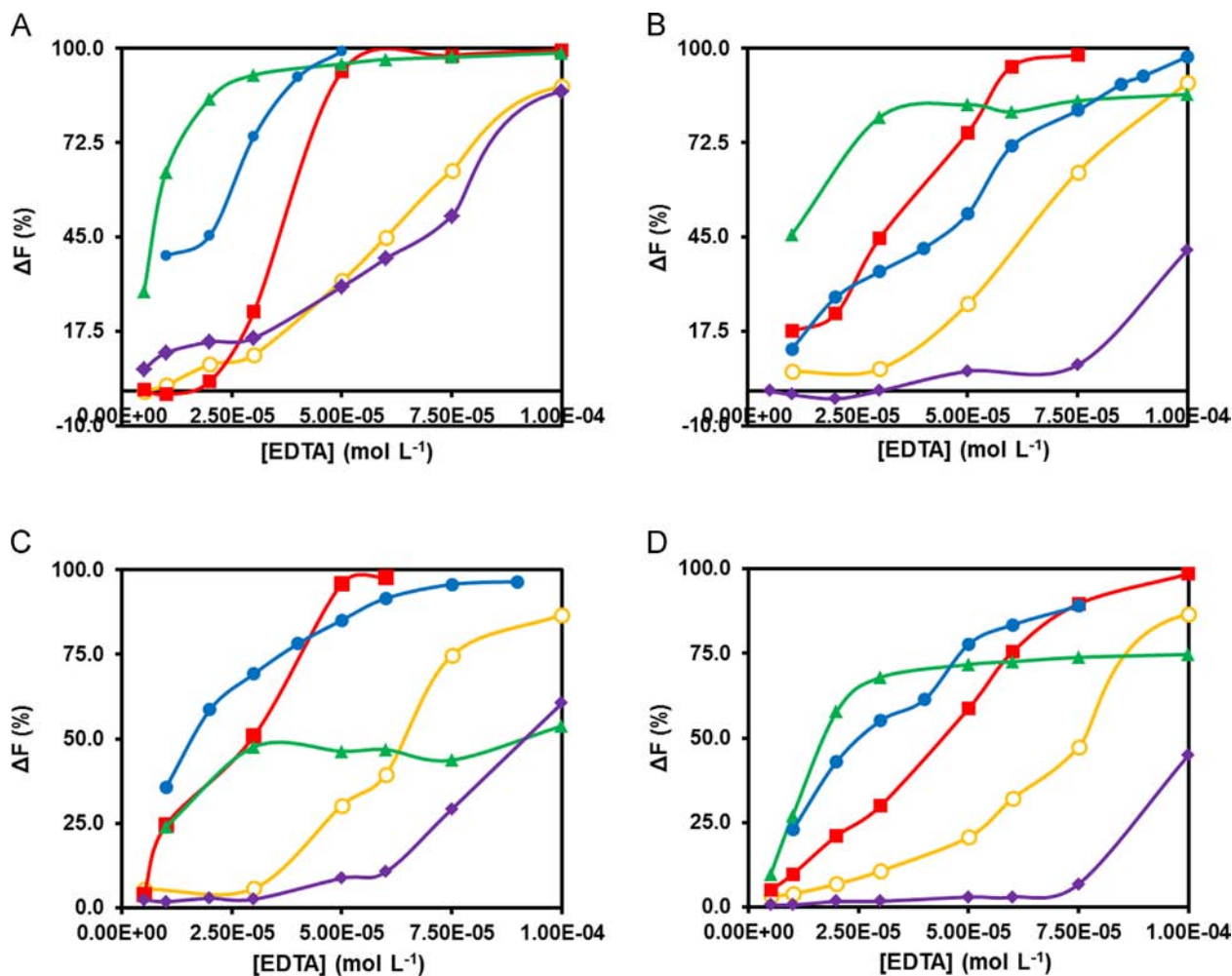


Fig. 4. Evaluation of the fluorescence quenching effect upon the interaction of EDTA, at different concentrations levels, to the synthesized QDs capped with different organic ligands: (●) CYS; (▲) GSH; (■) TGA; (○) MPA; (◆) MES, at different pH values: (A) pH 7; (B) pH 9; (C) pH 11; (D) pH 12.

Aiming at attaining high sensitivity and low detection limit the best combination of QDs and EDTA concentrations was selected by assaying increasing calcium concentrations of up to 4.0 mg L^{-1} and by plotting the respective calibration curves. 4.0 mg L^{-1} was chosen as the upper limit for the calcium concentration in order to ensure that the proposed methodology would allow obtaining a wide working concentrations range. Evaluation of the obtained results demonstrated that the calibration curve with the highest slope, thus guaranteeing higher sensitivity, was obtained when using a TGA–CdTe QDs concentration of $0.025 \text{ } \mu\text{mol L}^{-1}$ and an EDTA concentration of $4.0 \times 10^{-5} \text{ mol L}^{-1}$. Furthermore, slope values rapidly diminished for increasing QDs concentrations, tending subsequently for stabilization. This could be explained by an excess of nanocrystals, which, although affected by the quencher presence, exhibited a surplus of nanoparticles that guaranteed a fluorescence intensity that is only limited by inner filter effects (for too high concentrations). At low QDs concentrations, any slight variation in the quencher's concentration immediately results in a marked variation in the fluorescence response.

3.2.2. Optimization of the physical parameters

Since EDTA is mixed with the sample before reacting with the QDs solution, the extent of this reaction is clearly influenced by EDTA concentration, which is dependent of the dispersion undergone by the initial sample zone. The latter is determined by the operational flow parameters, namely the assayed volumes of QDs, EDTA and

sample solutions, reactor length and reaction time. The optimization of these parameters was carried out with the aim of attaining a compromise between reaction development and sample dispersion, maximizing the sensitivity of the developed method.

The influence of both the volumes of QDs solution and reactor length was simultaneously conducted. For each of the reactor's length studied, specifically 40, 50, 75 and 100 cm, the QDs volumes were varied between 30 and 90 μL , which corresponded to the insertion of a number of pulses between 3 and 9 (the stroke volume of each micro-pump was 10 μL). As it happened previously, the analytical signals were appraised through the slope of the calibration curves (sensitivity) obtained with Ca^{2+} solutions of up to 4.0 mg L^{-1} .

The results (Fig. 5) showed that the sensitivity of the methodology was enhanced with larger reactors, as the highest analytical signal was obtained with a 100-cm reactor, and with increasing volumes of sample, EDTA and QDs solutions. However, since for the 100-cm reactor the analytical signal approached stabilization at 7 pulses, or 70 μL , of each solution, these were the conditions that were selected for the subsequent assays.

The reaction time played a major role in terms of analytical signal magnitude, as it was already confirmed in the preliminary results. Since the residence time of the reaction zone within the analytical system prior to detection is determined by flow rate and reactor length it is possible to control the reaction time by adjustment of these parameters. Another possibility is to use a stopped flow strategy to increase residence time without affecting

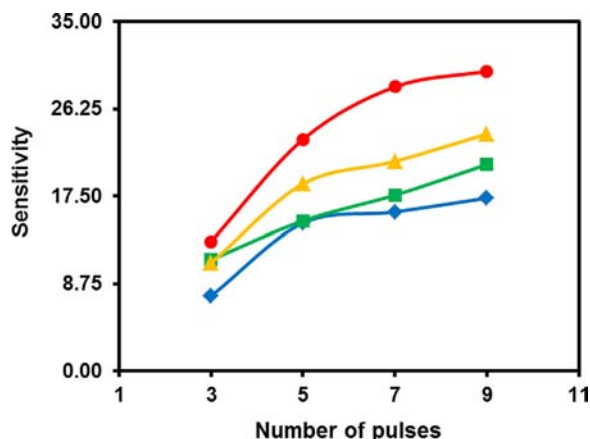


Fig. 5. Influence of the reactor's length and reagents and sample volumes (number of pulses of the corresponding micro-pump) on the sensitivity of the methodology. (◆) 40 cm; (■) 50 cm; (▲) 75 cm and (●) 100 cm.

sample dispersion. In this work the flow rate was fixed at 1.71 mL min^{-1} , which corresponded to the maximum working frequency of the micro-pumps (pulse time of 200 ms). In a MPFS the use of high flow rates combined with a pulsed flow results in an improved mixing of the solutions inside the flow tubing. Since the length of the reactor RC_2 (Fig. 1) was already optimized and fixed at 100 cm, the influence of the time of reaction was studied by exploiting a stopped flow approach [32]. This was achieved by stopping the flowing stream, therefore the sample zone (after the mixing of sample, EDTA and QDs solutions), in reactor RC_2 (Fig. 1) for 0, 30, 60, 90 and 120 s. The influence on the analytical signal was assessed by establishing calibration curves for Ca^{2+} concentrations of up to 4.0 mg L^{-1} .

The obtained results revealed that the sensitivity diminished with increasing stopped flow intervals. These results are in accordance with those observed in previous optimizations, namely the one concerning the reactor's length, confirming that a stopped flow approach did not favor reaction development. It could be anticipated that during the stopped flow interval the QDs deactivation process induced by EDTA led to a significant decrease in the nanocrystals stability that results in a pronounced fluorescence decrease.

3.3. Analytical features and application

By using the optimized physical and chemical conditions the developed methodology was evaluated in terms of the linear working range, limit of detection, determination rate, precision and accuracy. Additionally, the influence of some possible interfering species was tested before application to drinking waters.

3.3.1. Figures of merit

The study of the linear concentration range was carried out through the evaluation of the increase in the fluorescence signal versus blank signal (established from the simple interaction between QDs and EDTA) observed with increasing concentrations of calcium ions of up to 8.0 mg L^{-1} . A linear relationship between the fluorescence signal and the logarithmic of Ca^{2+} concentration was verified for concentration values ranging from 0.80 to 3.20 mg L^{-1} . The typical analytical curve was represented by the equation (Eq. (4)):

$$F = 43(\pm 2) \times \log C + 9.9(\pm 0.5) \quad (4)$$

in which F was the difference in fluorescence signal between sample and blank and C was the Ca^{2+} concentration, with a correlation coefficient of 0.9969 ($n=7$). The detection limit

calculated from the equation of the calibration curve [33] was about 0.66 mg L^{-1} . The developed methodology allowed a determination rate of about 62 h^{-1} and the analysis of about 20 samples per hour, considering the time required for the sample replacement and preparation of the automatic system.

3.3.2. Application to drinking waters

In order to apply the developed methodology to the determination of calcium ions in natural mineral waters, the influence of some cations that are usually present in the sample, namely magnesium, sodium and potassium, was assessed. Different sample solutions containing a fixed amount of Ca^{2+} (2.0 mg L^{-1}) and different quantities of the possible interferences under evaluation were analyzed by the developed methodology. A cation was considered as non-interfering if the analytical signal variation was inferior to 5% when compared to the analytical signal obtained in its absence. The results revealed that sodium and potassium did not interfere up to a 100-fold mass ratio regarding calcium concentration. Mg^{2+} can interfere if present at a mass concentration higher than 4-fold the Ca^{2+} . Since the amount of Mg^{2+} present in water samples did not exceed 4 fold the Ca^{2+} concentration, it was not considered interfering species. On the other hand, heavy metals could be considered potential interferences. However, the regulatory legislation established strict limits in terms of drinking water quality forbidding the occurrence of these species. Therefore, the study of these cations in the referred samples was considered dispensable.

Aiming at the validation of the proposed methodology, six samples consisting of mineral drinking waters and obtained in the Spanish commercial market, were analyzed by the QDs-based automatic methodology and the obtained results were compared with those provided by a widely recognized reference procedure [1], recommended by the Standard Methods Committee which is usually employed in routine analysis. This procedure involved a titration of calcium with EDTA using eriochrome blue black R as indicator under alkaline conditions.

Results obtained by both procedures are compiled in Table 3 and showed a good agreement, with relative deviations between -4.13 and 3.20% . A statistical analysis was also used for comparing the results in terms of precision and accuracy and was performed by application of a variance ratio F -test and a paired Student's t -test [33], respectively. The paired Student's t -test confirmed that there were no statistical differences between both methods, since the calculated value of t (0.45) was lower than the critical tabulated value ($t=2.57$) taking into account 2 degrees of freedom, for a confidence level of 95% ($n=6$). In relation to the evaluation of the precision through the application of the variance ratio F -test, it was

Table 3

Comparison of the analytical results obtained in the determination of calcium in commercial mineral waters samples by the proposed flow methodology and the reference method.

Sample	Declared Amount (mg L^{-1})	Amount found (mg L^{-1})		R.D % ^b
		MPFS methodology ^a	Reference method	
Perrier [®]	160	158 ± 3	162 ± 2	-2.67
Veri [®]	71.3	72 ± 2	72.8 ± 0.8	-0.78
Aquabona [®]	90.4	91 ± 3	88.9 ± 0.9	2.18
Solares [®]	75.2	73 ± 2	75.7 ± 0.8	-4.13
Fontvella [®]	86.1	87 ± 2	87 ± 2	0.13
Fontcabras [®]	90.1	92 ± 3	89 ± 1	3.20

^a Mean $\pm t_{0.05}$ (Student's t test) $\times (S/\sqrt{n})$.

^b Relative deviation of the developed method regarding the reference procedure.

observed that there were no significant differences between the results obtained by both procedures ($F_{\text{calculated}}=1.09$, $F_{\text{tabulated}}=5.05$), for a confidence level of 95%. Thus, the null hypothesis was verified and there was no significant difference between the proposed and the reference methodologies with respect to accuracy and precision, for a confidence level of 95%.

Finally, the evaluation of the intramethod precision through the repeated analysis of sample solutions (three consecutive determinations for each sample), revealed a good repeatability, taking into account the calculated concentration ranges for a confidence level of 95% (Table 3).

3.4. Quenching mechanism of TGA–CdTe QDs upon interaction with EDTA

Aiming at better understanding what occurs on the interaction between the TGA capped CdTe QDs and EDTA, some batch assays involving steady state fluorescence and UV–vis absorbance spectroscopy measurements were performed. These batch assays involved the preparation of several solutions containing $0.1 \mu\text{mol L}^{-1}$ of TGA–QDs and increasing concentrations of EDTA, ranging from 0.0 to $5.0 \times 10^{-5} \text{ mol L}^{-1}$. The fluorescence emission and absorbance spectra of the different solutions were monitored between 420 nm and 670 nm.

The results showed (Fig. 6(B)), as expected, that the fluorescence intensity of CdTe QDs was significantly quenched by the addition of increasing concentration of EDTA. Additionally, both absorption and fluorescence emission spectra revealed no shift of the wavelengths of maximum absorbance and emission (Fig. 6(A) and (B)).

The fluorescence quenching intensity data were also analysed by the Stern–Volmer equation in order to identify if the photoluminescence of QDs was quenched by EDTA through dynamic or static process. The characteristic feature of the Stern–Volmer plot obtained in this study was an upward curvature, concave towards the y-axis. This modified form of the Stern–Volmer equation is third order ($R=0.9996$) which was described as following:

$$\frac{F_0}{F} = 9.0 \times 10^{14}[\text{EDTA}]^3 + 4.0 \times 10^{10}[\text{EDTA}]^2 + 3.9 \times 10^5[\text{EDTA}] + 0.57 \quad (5)$$

in which F_0 and F are the fluorescence intensity in the absence and presence of the quencher EDTA, respectively. Under these circumstances it can be concluded that the fluorescence of TGA–CdTe QDs can be quenched by different mechanisms that rely mostly on collision phenomena and complex formation. However, for lower quencher concentrations the dependence of F_0/F on $[\text{EDTA}]$ was

linear, evidencing that for EDTA concentrations up to $2.5 \times 10^{-5} \text{ mol L}^{-1}$ only one type of quenching occurs. In that case the Stern–Volmer equation was described by:

$$\frac{F_0}{F} = 4.9 \times 10^4[\text{EDTA}] + 0.98, \quad (R = 0.9965) \quad (6)$$

Thus, in order to discriminate what type of quenching occur, some assays were performed to evaluate the temperature dependence of the Stern–Volmer quenching constant. The obtained results (Fig. S2 Supplementary material) demonstrated that the Stern–Volmer quenching constant (slope) decreased as the temperature increased. Indeed, higher temperatures favoured the dissociation of weakly bound complexes which are no longer prone to react and result, consequently, in lower quenching efficiency [34]. Based on these results it can be concluded that the static quenching mechanism played a major role in the interaction between the QDs and EDTA with concentration of up to $2.5 \times 10^{-5} \text{ mol L}^{-1}$.

The conclusions drawn from these assays corroborate the quenching mechanism proposed by Wu et al. [21] for the interaction between CdTe QD and EDTA. It is referred that the chelating reagent breaks the complex layer (Cd–capping ligand) and separates the Cd^{2+} from the QDs surface which is complexed by EDTA yielding a new complex Cd–EDTA. This ligand-detaching process induces the destabilization of the nanoparticles causing a significant fluorescence quenching of QDs.

3.5. Mechanism of the determination of free calcium ions

The determination of free calcium ions was based on the monitoring of the enhancement of the QDs fluorescence previously quenched upon the interaction with EDTA in aqueous solution. As aforementioned, the EDTA was used as a ligand-detaching agent that induced the surface depassivation of the TGA-capped CdTe QDs thus yielding nanoparticles with quenched photoluminescence properties. Thus, in the absence of free Ca^{2+} all EDTA was available for surface depassivation of the QDs and the obtained signal was minimum (blank signal, almost zero). On the contrary, in the presence of Ca^{2+} most EDTA formed a complex with free calcium ions (Ca–EDTA) and the number of EDTA molecules available to complex Cd^{2+} at the QDs surface decreased. The surface depassivation of the QDs is therefore reduced and the fluorescence quenching effect is restrained (enhancing of analytical signal). The observed fluorescence enhancing signal compared to the blank reading was used to quantify the amount of free calcium ions in mineral waters.

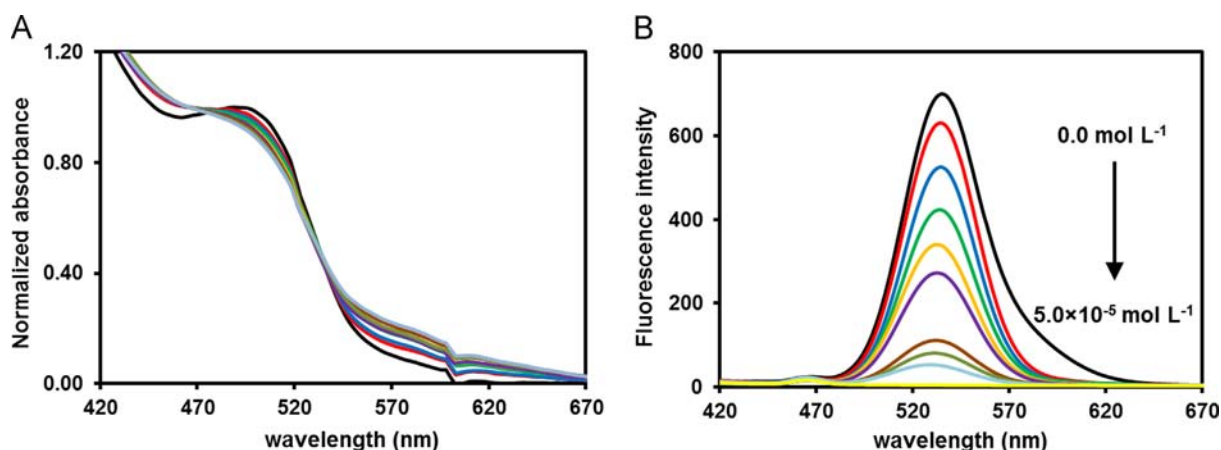


Fig. 6. (A) Normalized UV–vis absorbance and (B) fluorescence emission spectra of $0.1 \mu\text{mol L}^{-1}$ TGA–CdTe in the presence of different EDTA concentrations.

4. Conclusions

In this work, and for the first time, the interaction between EDTA and CdTe QDs capped with different organic ligands was evaluated and it was observed that the fluorescence quenching effect of EDTA on the nanoparticles was noticeably affected by the nature of the capping ligand and also by the pH of the reaction media. The CdTe QDs capped with TGA as organic ligand showed the highest reactivity (at pH=9.0). It was also observed that the fluorescence quenching of QDs could be explained by both dynamic and static mechanisms wherein for lower EDTA concentrations only the static process was verified. This observation confirmed the ligand-depletion mechanism in which EDTA promotes the breakage of the Cd–TGA binding at the surface of QDs yielding a new Cd–EDTA complex in solution. The EDTA-induced photoluminescent quenching of TGA–CdTe QDs was successfully used as a fluorescence sensing scheme for the calcium determination in drinking waters. This analytical procedure was automated in a micro-flow system exploiting the multipumping concept thus allowing an efficient and reliable determination of calcium. In comparison to the EDTA titrimetric method recommended by Standard Methods Committee, the proposed methodology allowed obtaining higher sample throughput and a noteworthy reduction in reagents consumption with consequent minimization of waste generation, circumventing, at same time, the main drawback related to the operational errors regarding the detection of the titration end-point.

Acknowledgements

S. Sofia M. Rodrigues thanks the “Fundação para a Ciência e Tecnologia” and FSE (Quadro Comunitário de Apoio) for the Ph.D. grant (SFRH/BD/70444/2010). This work received financial support from the European Union (FEDER funds through COMPETE) and National Funds (FCT, Fundação para a Ciência e Tecnologia) through project Pest-C/EQB/LA0006/2013. The work also received financial support from the European Union (FEDER funds) under the framework of QREN through Project NORTE-07-0124-FEDER-000067. To all financing sources the authors are greatly indebted.

Appendix A. Supporting information

Supplementary data associated with this article can be found in the online version at <http://dx.doi.org/10.1016/j.talanta.2014.11.008>.

References

- [1] A.P.H. Association, Part 3000 Metals (3500-Ca Calcium), in: L.S. Clesceri, A.E. Greenberg, A.D. Eaton (Eds.), *Standard Methods for the Examination of Water and Wastewater*, 1998, pp. 63–64.
- [2] J. Saurina, E. López-Aviles, A. Le Moal, S. Hernández-Cassou, *Anal. Chim. Acta* 464 (2002) 89–98.
- [3] M. Maj-Zurawska, M. Rouilly, W.E. Morf, W. Simon, *Anal. Chim. Acta* 218 (1989) 47–59.
- [4] Z. Chen, M.A. Adams, *Talanta* 47 (1998) 779–786.
- [5] A.N. Araújo, R.C.C. Costa, J.L.F.C. Lima, B.F. Reis, *Anal. Chim. Acta* 358 (1998) 111–119.
- [6] D.L. Smith, J.S. Fritz, *Anal. Chim. Acta* 204 (1988) 87–93.
- [7] R. García-Fernández, J.I. García-Alonso, A. Sanz-Medel, *J. Chromatogr. A* 1033 (2004) 127–133.
- [8] B. Paull, M. Macka, P.R. Haddad, *J. Chromatogr. A* 789 (1997) 329–337.
- [9] E. Gómez, J.M. Estela, V. Cerdà, *Anal. Chim. Acta* 249 (1991) 513–518.
- [10] A. Lopez-Molinero, V. Tejedor Cubero, R. Domingo Irigoyen, D. Sipiera Piazuelo, *Talanta* 103 (2013) 236–244.
- [11] T. Yamane, E. Goto, *Talanta* 38 (1991) 139–143.
- [12] F. Blasco Gómez, F. Bosch Reig, P. Campins Falcó, *Talanta* 49 (1999) 155–163.
- [13] M.A. Gil Libarona, F.A. Iníón, *Anal. Chim. Acta* 536 (2005) 159–169.
- [14] M.E. Khalifa, *Chem. Anal. (Warsaw)* 41 (1996) 357–362.
- [15] C. Frigerio, D.S.M. Ribeiro, S.S.M. Rodrigues, V.L.R.G. Abreu, J.A.C. Barbosa, J.A.V. Prior, K.L. Marques, J.L.M. Santos, *Anal. Chim. Acta* 735 (2012) 9–22.
- [16] W.R. Algar, A.J. Tavares, U.J. Krull, *Anal. Chim. Acta* 673 (2010) 1–25.
- [17] I. Costas-Mora, V. Romero, I. Lavilla, C. Bendicho, *TrAC, Trends Anal. Chem.* 57 (2014) 64–72.
- [18] S. Chen, J. Tian, Y. Jiang, Y. Zhao, J. Zhang, S. Zhao, *Anal. Chim. Acta* 787 (2013) 181–188.
- [19] X.Y. Hu, K. Zhu, Q.S. Guo, Y.Q. Liu, M.F. Ye, Q.J. Sun, *Anal. Chim. Acta* 812 (2014) 191–198.
- [20] R. Gui, X. An, H. Su, W. Shen, Z. Chen, X. Wang, *Talanta* 94 (2012) 257–262.
- [21] P. Wu, X.P. Yan, *Chem. Commun.* 46 (2010) 7046–7048.
- [22] Z. Tang, Y. Wang, S. Shanbhag, N.A. Kotov, *J. Am. Chem. Soc.* 128 (2006) 7036–7042.
- [23] R.A.S. Lapa, J.L.F.C. Lima, B.F. Reis, J.L.M. Santos, E.A.G. Zagatto, *Anal. Chim. Acta* 466 (2002) 125–132.
- [24] D.D. Perrin, B. Dempsey, *Buffers for pH and Metal Ion Control*, Chapman & Hall, Inc, New York, 1974.
- [25] H. Qian, C. Dong, J. Weng, J. Ren, *Small* 2 (2006) 747–751.
- [26] L. Zou, Z. Gu, N. Zhang, Y. Zhang, Z. Fang, W. Zhu, X. Zhong, *J. Mater. Chem.* 18 (2008) 2807–2815.
- [27] Y.-h. Zhang, H.-s. Zhang, M. Ma, X.-f. Guo, H. Wang, *Appl. Surf. Sci.* 255 (2009) 4747–4753.
- [28] C.I.C. Silvestre, C. Frigerio, J.L.M. Santos, J.L.F.C. Lima, *Anal. Chim. Acta* 699 (2011) 193–197.
- [29] N. Gaponik, D.V. Talapin, A.L. Rogach, K. Hoppe, E.V. Shevchenko, A. Kornowski, A. Eychmüller, H. Weller, *J. Phys. Chem. B* 106 (2002) 7177–7185.
- [30] W.W. Yu, L. Qu, W. Guo, X. Peng, *Chem. Mater.* 15 (2003) 2854–2860.
- [31] C. Liang-Yih, T. Chia-Hung, C. Hung-Lung, C. Ching-Hsiang, *Surface modification of CdSe and CdS quantum dots-experimental and density function theory investigation*, in: *Nanocrystals—Synthesis, Characterization and Applications*, 2012, pp. 149–168.
- [32] J. Růžička, E.H. Hansen, *Anal. Chim. Acta* 106 (1979) 207–224.
- [33] J.N. Miller, J.C. Miller, *Statistics and Chemometrics for Analytical Chemistry*, sixth ed., Prentice Hall/Pearson, England, 2010.
- [34] J.R. Lakowicz, *Quenching of fluorescence*, in: J.R. Lakowicz (Ed.), *Principles of Fluorescence Spectroscopy*, Springer, US, 2006, pp. 277–330.